Angle-resolved photoemission study of Sr_2RuO_4

T. Yokoya, A. Chainani, and T. Takahashi
Department of Physics, Tohoku University, Sendai 980-77, Japan

H. Ding and J. C. Campuzano
Material Science Division, Argonne National Laboratory, 9700 South Cass Avenue, Argonne, Illinois 60439
and Department of Physics, University of Illinois at Chicago, 845 West Taylor Street, Chicago, Illinois 60607

H. Katayama-Yoshida
Department of Physics, Tohoku University, Sendai 980-77, Japan
and Institute of Science and Industrial Research, Osaka University, Ibaraki, Osaka 567, Japan

M. Kasai
Joint Research Center for Atom Technology (JRCAT), Tsukuba, Ibaraki 305, Japan

Y. Tokura
Joint Research Center for Atom Technology (JRCAT), Tsukuba, Ibaraki 305, Japan
and Department of Applied Physics, The University of Tokyo, Tokyo 113, Japan

We present high-resolution (HR) angle-resolved photoemission spectroscopy (ARPES) measurements of the noncuprate layered perovskite superconductor Sr_2RuO_4. ARPES spectra of the whole valence-band region obtained along two high-symmetry directions in the Brillouin zone show clear dispersion, generally similar to that of a band calculation. However, HRARPES measurements taken in the vicinity of the Fermi level (E_F) show narrower $Ru4d\varepsilon(xy,yz,zx)$-$O2p\pi$ antibonding bands than those predicted by the band calculation. More significantly, there is an extended van Hove singularity very close to E_F ($E_B=11$ meV) along the Ru-O bonding direction, which is known to exist in cuprate high-temperature superconductors. The Fermi-surface topology obtained by HRARPES (one electronlike Fermi surface sheet centered at the Γ point and two holelike sheets centered at the X point) is different from the band calculation (two electronlike sheets centered at the Γ point and one holelike sheet centered at the X point), although the electron count is the same in both cases. These results suggest that electron-electron correlations cause the modification of the Fermi-surface topology, and is thus necessary for understanding the electronic structure and properties of Sr_2RuO_4. [S0163-1829(96)02642-2]

I. INTRODUCTION

It is generally accepted that the CuO_2 plane in high-temperature superconductors (HTSC's) plays a fundamental role in the occurrence of superconductivity at such high temperatures, since every HTSC has CuO_2 planes as a common structural element. The recent discovery of superconductivity at 1 K in the noncuprate layered perovskite oxide Sr_2RuO_4 (Ref. 1) would provide a unique opportunity to study the role of CuO_2 planes in HTSC's. Further, since Sr_2RuO_4 has a temperature-squared (T^2) dependence of the electrical resistivity at low temperatures in contrast to the T-linear behavior observed in HTSC's, a comparative study would give an important insight into the mechanism of the anomalous normal-state properties of HTSC's.

The most essential difference in the electronic structure near the Fermi level (E_F) between the ruthenate and the cuprates is that the bands which cross E_F are of $Ru4d\varepsilon(xy,yz,zx)$-$O2p\pi$ antibonding character[2,3] in Sr_2RuO_4, while those in the cuprates are of $Cu3dx^2$-y^2-$O2p\sigma$ antibonding nature. This is due to the difference in the number of d electrons in the outermost shell; a

Ru atom in Sr_2RuO_4 has four $4d$ electrons while a Cu atom in HTSC's has nine $3d$ electrons. The band-structure calculation[2,3] has predicted that the Fermi surface of Sr_2RuO_4 consists of two electronlike cylindrical sheets around the Γ point and one holelike sheet at the X point in the Brillouin zone,[2,3] while the calculated Fermi surface of La_2CuO_4 consists of only one holelike sheet centered at the X point.[4] The normal-state resistivity of Sr_2RuO_4 is found to be highly anisotropic between the in-plane and the out-of-plane component,[1,5] but both show a T^2 dependence below 25 K characteristic of a typical Fermi liquid.[1] The magnetic measurements show an enhanced Pauli paramagnetism;[6-8] the measured specific heat, 39–45 mJ/K^2 mol, is four times larger than the calculated value[1,6] which suggests that the correlation effect plays an important role in Sr_2RuO_4. A recent resonant photoemission study of Sr_2RuO_4 has reported the existence of a correlation-induced satellite which is remarkably enhanced at the Ru $4p$-$4d$ core threshold.[9]

In this paper we report a comprehensive high-resolution (HR) angle-resolved photoemission spectroscopy (ARPES) on a single-crystal Sr_2RuO_4. This extends our previous study[10] which showed the important similarity to the

HTSC's. Our previous measurements found the existence of an extended van Hove singularity (vHS) in this material.[10] Here we show comprehensive sets of ARPES data of this extended vHS measured with a higher-energy resolution. We also study the entire valence-band structure and compare the experimental results with the band-structure calculation.[2,3] We observe three groups of dispersive bands; one near E_F, one around 3-eV binding energy, and a third at 6–8 eV binding energy. These are attributed to the Ru$4d\varepsilon$-O2$p\pi$ antibonding bands, the Ru$4d\varepsilon$-O2$p\pi$ nonbonding bands, and the Ru$4d\varepsilon$-O2$p\pi$ bonding bands, respectively. This structure is qualitatively similar to that of the band-structure calculation.[2,3] However, HRARPES measurements near E_F have revealed that a vHS exists just below E_F over a wide region of the Brillouin zone, in a remarkably similar manner to the extended vHS observed in the HTSC's.[11–15] Such an extended vHS just *below* E_F has not been predicted by band calculations[2,3] in either the ruthenate or the cuprate, though Singh[3] has predicted that a simple (notextended type) vHS exists at about 60 meV *above* E_F at approximately the same position in the Brillouin zone.

We have measured a number of HRARPES spectra along many cuts in the Brillouin zone and thus mapped out the Fermi surface, which was found to consist of one electron-like cylindrical sheet centered at the Γ point and two holelike ones centered at the X point. The larger holelike sheet forms the extended vHS around the middle point between the Γ and Z points. Thus, the shape of the observed Fermi surface is substantially different from that of the band calculation,[2,3] which has predicted two electronlike sheets centered at the Γ point and one holelike sheet centered at the X point. However, the total electron count estimated by the HRARPES measurement was found to be almost the same as that of the band calculation, suggesting a compensation effect due to the Luttinger theorem.[16] We discuss some possible origins to bring about the difference in the Fermi-surface topology between the experiment and the calculation. We also discuss the proposed conjecture[11,14] that the position of the extended vHS with respect to E_F has a close relation to the T-linear dependence of resistivity observed in HTSC's.

II. EXPERIMENT

Photoemission spectroscopy was performed on several single crystals prepared by the floating zone method. X-ray diffraction was used to characterize the structure of the samples. Magnetic susceptibility measurements confirmed that superconductivity occurs below 0.9 K, as reported earlier.[1] The crystal orientation was determined by Laue backscattering before mounting the sample in the spectrometer.

Valence-band ARPES measurements using He I photons (21.2 eV) with an energy resolution of 50 meV and an angular acceptance of $\pm 1°$ were performed at Tohoku University. Samples were cleaved *in situ* and measured at 20 K in a vacuum better than 5×10^{-11} Torr. All measurements were carried out within 4 h after cleaving the sample, because the sample surface showed signs of degradation a few (6–7) h after cleaving, as seen by the reduction in intensity of the sharp peak near E_F and a concomitant growth of the well-known contamination or degradation derived feature at about

10-eV binding energy.[17] In valence-band measurements, the Fermi level was referred to that of a gold film deposited onto the sample mounting substrate. High-energy-resolution ARPES measurements near E_F were carried out at the Synchrotron Radiation Center, Wisconsin, using a 4-m normal incidence monochromator. The total energy resolution (photons and electrons) was 20 meV and the angular acceptance window was $\pm 1°$. A higher-energy resolution measurement ($\Delta E = 15$ meV) was performed in order to determine the accurate position of the extended vHS. The measurements with synchrotron radiation were performed at 13 K also within a few hours after cleaving the sample. A Pt foil which was in electrical contact with the sample was used as a Fermi level reference.

We have measured ARPES spectra of more than ten crystals and confirmed the reproducibility of the ARPES spectra by measuring and comparing the normal emission spectrum for each sample. The samples used in this study are numbered serially. We measured a number of ARPES spectra by changing the polar and azimuthal angles in the c plane (cleaved plane) of the crystal. Polar and azimuthal angles are directly related to positions in the Brillouin zone. All ARPES spectra are labeled in terms of the values of (k_x, k_y), where k_x and k_y are the wave vectors parallel to the Ru-O bonding direction (in units of Å^{-1}). Since Sr_2RuO_4 has a body-centered tetragonal crystal structure,[1] k_x and k_y are equivalent to each other.

III. RESULTS AND DISCUSSION

A. Valence band

Figure 1 shows the valence-band ARPES spectra of Sr_2RuO_4 along the ΓX and ΓZ high-symmetry directions in the Brillouin zone measured at 20 K using the He I resonance line (21.2 eV). The ΓZ direction corresponds to the Ru-O bonding direction in the crystal while the ΓX direction is 45° away from it. We used two different samples for the two different directions (samples no. 1 and no. 2 for the ΓX and ΓZ directions, respectively). Note that the normal emission ($k_x = k_y = 0$) spectra from the two different samples are almost identical to each other, which indicates a high reproducibility in the present ARPES measurements. We find in Fig. 1 that the ARPES spectra in both directions exhibit several prominent features over a wide binding energy range of 10 eV from E_F and their intensity and position change very sensitively with the wave vectors k_x and k_y. These spectral changes directly represent the band structure of Sr_2RuO_4. All ARPES spectra have well-separated three main structures located at E_F, 2–4 eV, and 6–8 eV, respectively. The structure around 6–8 eV is ascribed to the Ru$4d\varepsilon$-O2$p\pi$ bonding states, which form a very sharp single peak at the Γ point ($k_x = k_y = 0$), but appear to separate into several bands when k_x and/or k_y are increased as shown in Fig. 1. This change of the position of peaks in the ARPES spectrum with respect to the values of (k_x, k_y) indicates a substantial energy dispersion of the Ru$4d\varepsilon$-O2$p\pi$ bonding states. On the other hand, the feature around 3 eV in the ARPES spectra, which is assigned to the Ru$4d\varepsilon$-O2$p\pi$ nonbonding states, shows very small energy dispersion but a drastic change in intensity with changing wave vector. The small peak near E_F is attributed to the Ru$4d\varepsilon$-O2$p\pi$ antibonding bands. It is located
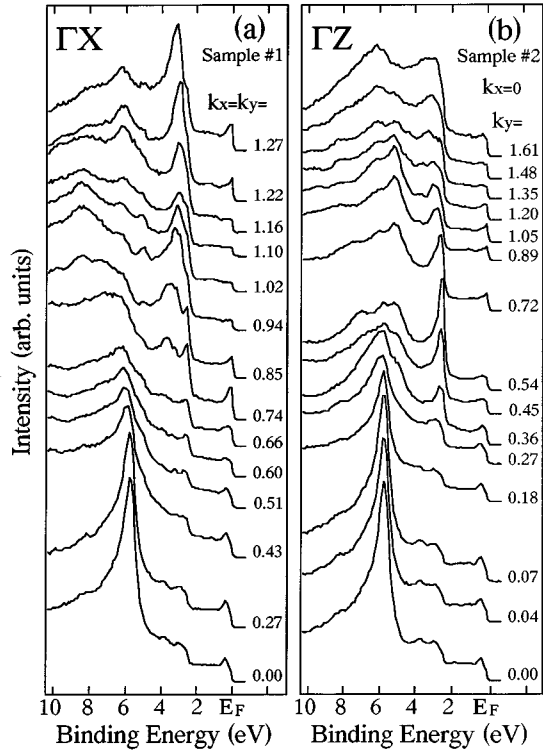
FIG. 1. Valence-band ARPES spectra of Sr_2RuO_4 (001) single-crystal surfaces measured with He I photons (21.2 eV) at 20 K along the two high-symmetry directions in the Brillouin zone, ΓX (a) and ΓZ (b). Each spectrum is labeled with a set of wave vectors (k_x, k_y) in units of Å^{-1} which indicates the position of the ARPES measurement in the Brillouin zone for electrons at E_F.
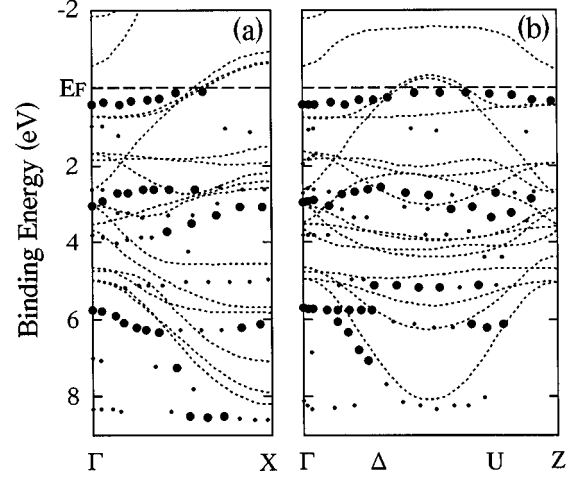

FIG. 2. Experimental band structure of Sr_2RuO_4 obtained by the present ARPES measurements shown in Fig. 1. Large and small filled circles represent strong and weak structures in the ARPES spectra, respectively. A band-structure calculation (Ref. 2) is also shown by dashed lines for comparison.

slightly away from E_F at the Γ point ($k_x = k_y = 0$), gradually approaches E_F with increasing wave vector, and finally appears to cross E_F at $k_x = k_y = 0.85$ in the ΓX direction, since the spectral intensity suddenly decreases at this point. After the band crosses E_F, the spectral intensity at E_F is quite small until $k_x = k_y = 1.16$, and recovers at $k_x = k_y = 1.22$. This suggests that the same band disperses below E_F in the second Brillouin zone. In contrast, the peak near E_F along the ΓZ direction [Fig. 1(b)] retains its intensity even after it touches E_F at $(k_x, k_y) = (0, 0.89)$. This shows a qualitative difference in the electronic structure near E_F between the two high-symmetry directions in the Brillouin zone.

Figure 2 shows the experimental band structure of Sr_2RuO_4 (filled large and small circles) obtained from the present ARPES measurements (Fig. 1) using the formula,[18] $k = [2m(\hbar\omega - E_B - \phi)/\hbar^2]^{-1/2}\sin\theta$, where k is the wave vector parallel to the high-symmetry direction, m the electron mass, E_B the binding energy, ϕ the work function, and θ the polar angle of photoemitted electrons with respect to the surface normal. In mapping out the experimental band structure we neglected the interlayer energy dispersion since the electronic structure of Sr_2RuO_4 has a strong two-dimensional character as expected from its crystal structure.[2,3] Actually, a negligible interlayer dispersion was observed in normal emission ARPES measurements with synchrotron radiation.[9] The experimental results are compared with the band calculation (broken lines) (Ref. 2) in Fig. 2.

B. Extended van Hove singularity

Figure 3 shows three sets of HRARPES spectra near E_F measured with two different sample surfaces (samples no. 3 and no. 4) in directions parallel to the ΓX and ΓZ lines as well as perpendicular to the ΓZ line in the Brillouin zone. Figure 4 shows the cuts in the Brillouin zone where the measurements shown in Fig. 3 were performed; open and filled circles denoted by $3a$–$3c$ in Fig. 4 correspond to sets of spectra in Figs. 3(a)–3(c), respectively.

In Figs. 3(a) and 3(b) we find a broad peak located at about 0.4 eV from E_F near the Γ point ($|k_x|, |k_y| < 0.10$ Å^{-1}) in the Brillouin zone, which is assigned to the Ru4$d\varepsilon$-O2$p\pi$ antibonding bands. In the ΓX direction [Fig. 3(a)], this band gradually approaches E_F with increasing (k_x, k_y) and finally appears to cross E_F near $(k_x, k_y) = (0.50, 0.65)$ since the spectral intensity at E_F suddenly decreases at this point. As a guide to the eyes, a possible dispersion of the prominent structure in the spectra is marked with a broken line. On the other hand, as shown in Fig. 3(b), this prominent band appears not to lose its intensity even after it touches E_F along the ΓZ direction (the Ru-O bonding direction). This shows a qualitative difference between the two high-symmetry directions in the Brillouin zone. As found in Fig. 3(b), the peak at E_F retains its intensity over a substantial part of the Brillouin zone, forming a very flat nondispersive band just below E_F between the Γ and Z points. In order to further characterize this flat band, we performed another set of HRARPES measurements perpendicular to the ΓZ direction as shown in Fig. 3(c). First, note that the two ARPES spectra obtained at the same point in the Brillouin zone [$(k_x, k_y) = (0.07, 0.85)$ in Figs. 3(b) and 3(c)] but with different crystal orientation agree with each other very well, indicating a good reproducibility from different scans, as well as a high crystal alignment accuracy. It is evident from Fig. 3(c) that the ARPES peak which forms a very flat band just below E_F in the ΓZ direction shows the opposite energy dispersion perpendicular to it. This indicates that the band forms a saddle point with a
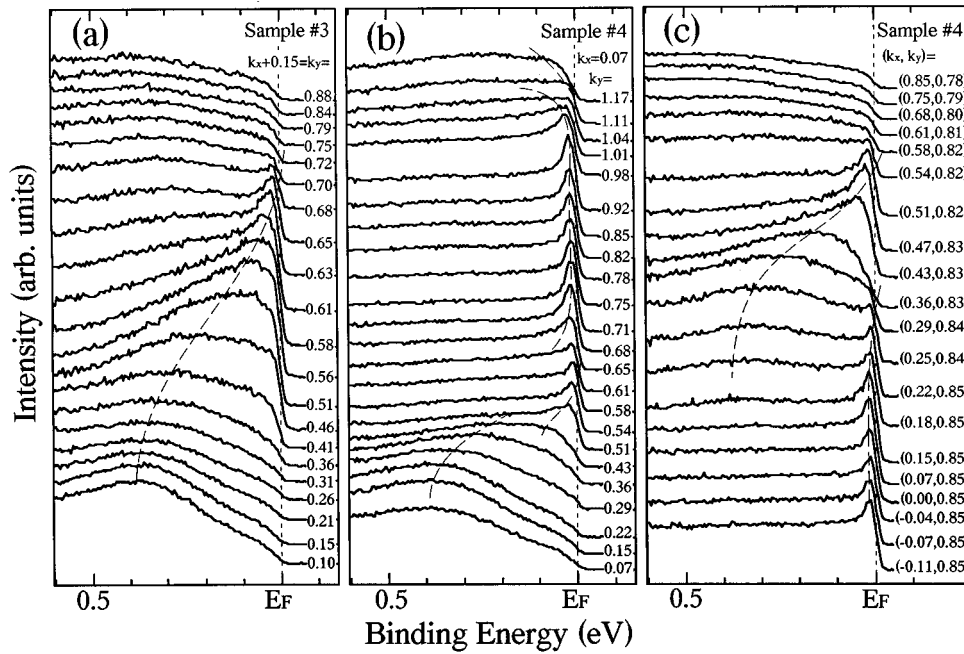
FIG. 3. High-resolution ARPES spectra near E_F along three directions parallel to (a) ΓX, (b) ΓZ, and (c) perpendicular to the ΓZ direction, measured at 13 K using 21.2-eV energy photons. Dashed lines are guide to the eyes.

substantial flat area around the middle point between the Γ and Z points in the Brillouin zone. We also find in Fig. 3(c) that another band approaches E_F from the high-binding energy side and crosses E_F at $(k_x,k_y)=(0.51,0.82)$. We confirmed that the spectral change with (k_x,k_y) is symmetric with respect to the ΓZ line.
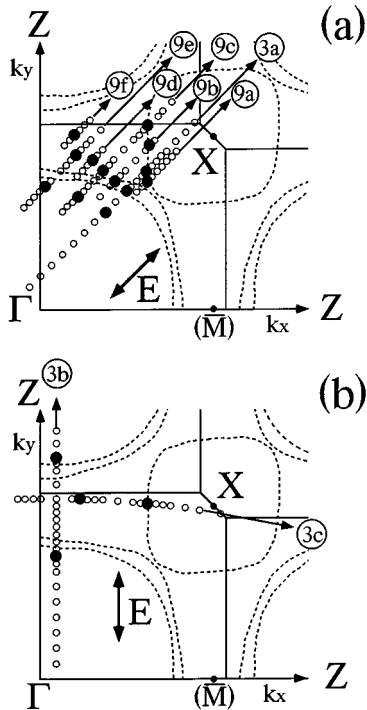
FIG. 4. Brillouin zone of Sr_2RuO_4. A set of circles denoted by number and alphabet represents a set of ARPES measurements in one cut in the Brillouin zone, which correspond to a set of ARPES spectra in Figs. 3 and 9. The E_F-crossing points are shown by filled circles. Also shown are the direction of polarization (E) of incident light in the ARPES measurements and the Fermi surface predicted by the band calculation (broken lines) (Ref. 2).

The experimental band structure of Sr_2RuO_4 near E_F obtained from the present ARPES measurements (Fig. 3) using the conventional method described above[18] is shown in Fig. 5. To determine the energy position of the band, we took the binding energy of the local maximum in the ARPES spectrum regardless of the width of peaks. However, in the case when more than two bands are accidentally situated very close to each other and form a very broad structure in the ARPES spectrum, we estimated the position of each band by comparing some adjacent ARPES spectra. The detailed procedure to determine the E_F-crossing point will be explained in the next section on Fermi surface topology. For comparison the band calculation[2] is also shown in Fig. 5. Although the ARPES measurements in Fig. 3 were performed in the cuts slightly away from the high-symmetry lines, the deviation is expected to be small. This is evident from the experimental fact that the two ARPES spectra in Fig. 3(c), one of which is on the ΓZ line $[(k_x,k_y)=(0.0,0.85)]$ and the other is slightly off from it $[(k_x,k_y)=(0.07$ or $0.15,0.85)]$ look almost identical to each other within the present energy resolution. In Fig. 5 we find that the observed band dispersion near E_F is almost two times smaller than that of the band calculation, suggesting a strong mass renormalization due to electron correlations in this material. This result is consistent with an optical measurement which found that the effective mass of the conduction carriers in Sr_2RuO_4 is about twice the calculated one.[19] More importantly, we found that the band near E_F has a flat maximum over a substantial range of k values along the ΓZ direction and also shows a flat minimum perpendicular to it, forming an extended saddle point. A similar extended van Hove singularity (vHS) has been observed in several cuprate HTSC's.[11–15] For example, a HRARPES study of $YBa_2Cu_4O_8$ (Y124) observed an extended vHS at 19-meV binding energy along the Cu-O bonding direction.[13]

In order to accurately determine the position of the extended vHS, we performed a higher-resolution measurement (15 meV total energy resolution) on sample no. 5 at the
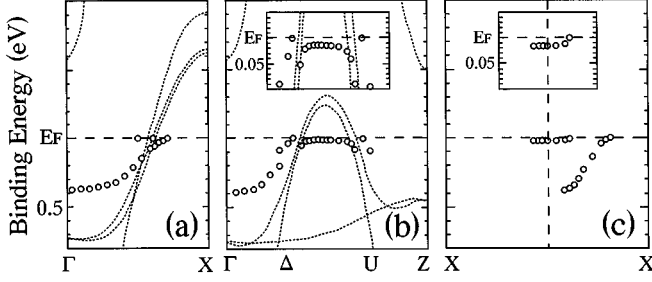
FIG. 5. Experimental band structure near E_F of Sr_2RuO_4 (open circles) determined by the present HRARPES measurements shown in Fig. 3. The band-structure calculation (Ref. 2) is shown by broken lines for comparison. Insets show the enlargement near E_F.

FIG. 6. A high-energy resolution ($\Delta E = 15$ meV) ARPES spectrum of Sr_2RuO_4 measured at 13 K at the middle point (M point) between the Γ and the Z point in the Brillouin zone. A HRPES spectrum of a Pt foil measured under the same condition is shown for a reference of the Fermi function. Note that the leading edge of the spectrum of Sr_2RuO_4 is sharper than the Fermi function, indicating that the peak is clearly below E_F.

middle point between the Γ and the Z points. We call this the M point in analogy to the HTSC cuprates. As shown in Fig. 6, the peak is found at 12 meV, and since its leading edge is sharper than the Fermi function as seen in the spectrum of Pt, it is clearly below E_F. In order to get a better estimate of the peak position, we fitted the peak to a spectral function using a Fermi-liquid line shape taking into account of the Fermi function and the known energy-resolution function of the spectrometer. The fitting indicates that the binding energy of this quasiparticle peak is approximately 11 meV. It is to be noticed here that the band calculation by Singh predicted a vHS located 60 meV *above* E_F but not of the extended type.[3] In order to compare the extended vHS in Sr_2RuO_4 to those in Y124 (Ref. 13) and $Bi_2Sr_2CaCu_2O_8$ (Bi2212) (Ref. 20), we list in Table I the width of the flat region along the ΓZ direction, the width of the vHS below E_F along the XX direction, and the binding energy of the vHS at the M point. It is shown in Table I that the width of the extended region along the ΓZ direction, namely the Ru-O direction, is about two times smaller in Sr_2RuO_4 than in the cuprates. In contrast, the width of the vHS below E_F along the XX direction is slightly larger in Sr_2RuO_4. It is also noticed that the energy position of the vHS is much closer to E_F in Sr_2RuO_4 than in the cuprates, meaning that the energy dispersion along the XX direction is much flatter in Sr_2RuO_4 than in the cuprates. All these indicate that the vHS in Sr_2RuO_4 extends along two directions, while the singularity in the HTSC's extends only along one direction. A simple vHS yields a logarithmic divergence in the density of states (DOS),[21] while an extended singularity yields a power-law divergence of the form $(E - E_c)^{-1/2}$, where E_c is the critical point
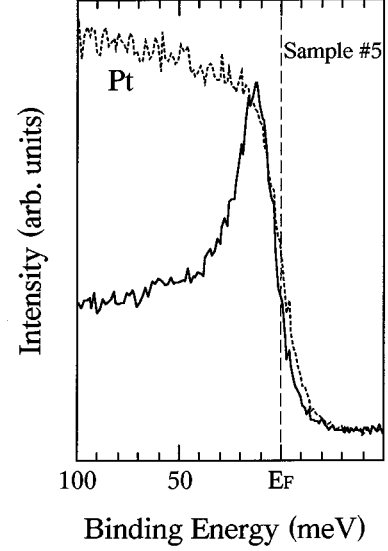
energy.[13] In the vHS scenario,[13,21] the enhancement of T_c comes from this divergence in the DOS. Here we find a vHS extending in two directions, which presumably would yield a δ-function singularity in the DOS, with weight equal to the area of the flat region. Such a singularity in Sr_2RuO_4 would make the transition temperature directly proportional to the pair potential. Furthermore, the critical energy of the singularity is closer to E_F than in the case of HTSC's, although Sr_2RuO_4 has a T_c of only 0.9 K. These observations raise important questions as to the validity of the simple vHS scenario for high temperature superconductivity.

The vHS scenario has also been used to explain some anomalous normal-state properties such as the T-linear resistivity in terms of the critical energy of the vHS.[21] For example, King *et al.*[11,14] have pointed out that $Nd_{2-x}Ce_xCuO_4$ shows a T^2-dependent resistivity with its vHS located about 350 meV below E_F, while $Bi_2(Sr_{0.97}Pr_{0.03})_2CuO_6$ and Bi2212 show a T-linear resistivity with the vHS' being just below E_F. However, in Sr_2RuO_4 this correlation does not hold,

TABLE I. Width of the flat region of vHS along the ΓZ direction, width of vHS below E_F along the XX direction, and binding energy of vHS at the middle point (M point) between the Γ point and the Z point for Sr_2RuO_4, $YBa_2Cu_4O_8$, and $Bi_2Sr_2CaCu_2O_8$.

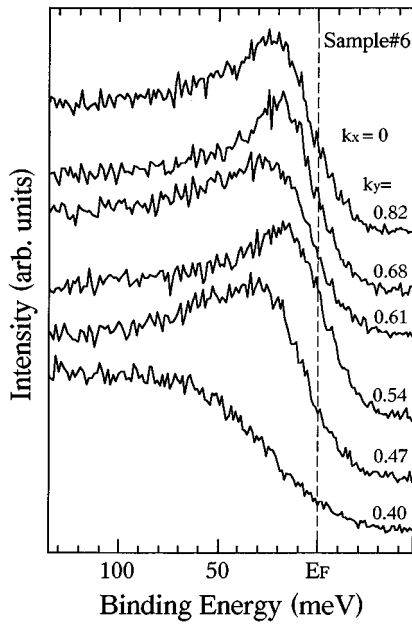| Samples	Width of flat region of vHS along ΓZ direction ($Å^{-1}$)	Width of vHS below E_F along XX direction ($Å^{-1}$)	Binding energy of vHS at M point (meV)
Sr_2RuO_4	0.27	0.35	11
$YBa_2Cu_4O_8$ (Ref. 13)	0.50	0.28	19
$Bi_2Sr_2CaCu_2O_8$ (Ref. 20)	0.45	0.30	34

FIG. 7. HRARPES spectra near E_F measured along the ΓZ direction, showing the case when several bands show dispersions near E_F and some of them cross it. A band approaches E_F from $k_y=0.4$ and appears to cross it at $k_y=0.54$ since the photoemission intensity at E_F shows a substantial decrease at $k_y=0.61$ and simultaneously the middle point of the leading edge shows a slight backward shift.

since the vHS is located much closer to E_F than those of the hole-doped HTSC cuprates, but shows a T^2 dependence of the resistivity at low temperatures. Therefore the simple explanation of anomalous normal-state properties in the vHS scenario has to be reexamined.

C. Fermi-surface topology

Since the extended vHS near E_F has not been predicted by band calculations,[2,3] the measured Fermi-surface topology

would be substantially different from the calculated one. We have performed HRARPES measurements at many points in the Brillouin zone to map out the Fermi surface in detail. Since the determination of the E_F-crossing point using ARPES has an inevitable ambiguity due to the finite energy and angular resolutions, we took the following criteria to determine the E_F-crossing point. In the case when one well-defined peak (or band) approaches E_F and appears to cross it, as seen by the drastic decrease of its intensity at E_F, we choose the point where the peak loses about a half of its intensity, taking into account of the background. This is the case for $(k_x,k_y)=(0.50,0.65)$ in Fig. 3(a). However, when several bands move together to E_F, we cannot apply this criterion. In this case we used the variation of photoemission intensity at E_F to determine the E_F-crossing point. Figure 7 shows a typical example for this case. The ARPES measurement is along the ΓZ line at an energy resolution of 15 meV with sample no. 6. As is seen in Fig. 7, a band gradually approaches E_F from $k_y=0.40$ and appears to cross E_F at $k_y=0.54$. However, the intensity of a peak at E_F does not show a drastic decrease, since another band also appears to move to E_F just after the first one. It is clear that in this case we cannot use the criterion described above. As seen in Fig. 7, the photoemission intensity at E_F gradually increases from $k_y=0.40$ to $k_y=0.54$, where the middle point of the Fermi-edge cutoff is located slightly above E_F. When we further increase the wave vector to $k_y=0.61$, the photoemission intensity at E_F decreases compared with that at $k_y=0.54$ and simultaneously the middle point of the Fermi-edge cutoff moves backward slightly. This indicates that the band certainly crosses E_F at $k_y=0.54$. We applied this criterion to the ARPES spectra in Fig. 3 (the enlargement near E_F is shown in Fig. 8) as well as in Fig. 9, where we show another six sets of HRARPES spectra in the vicinity of E_F measured for several cuts in the Brillouin zone using sample no. 3. The position of the cuts in the Brillouin zone where the ARPES measurements were done is seen in Fig. 4; the correspondence between the ARPES spectra and the cut is identified
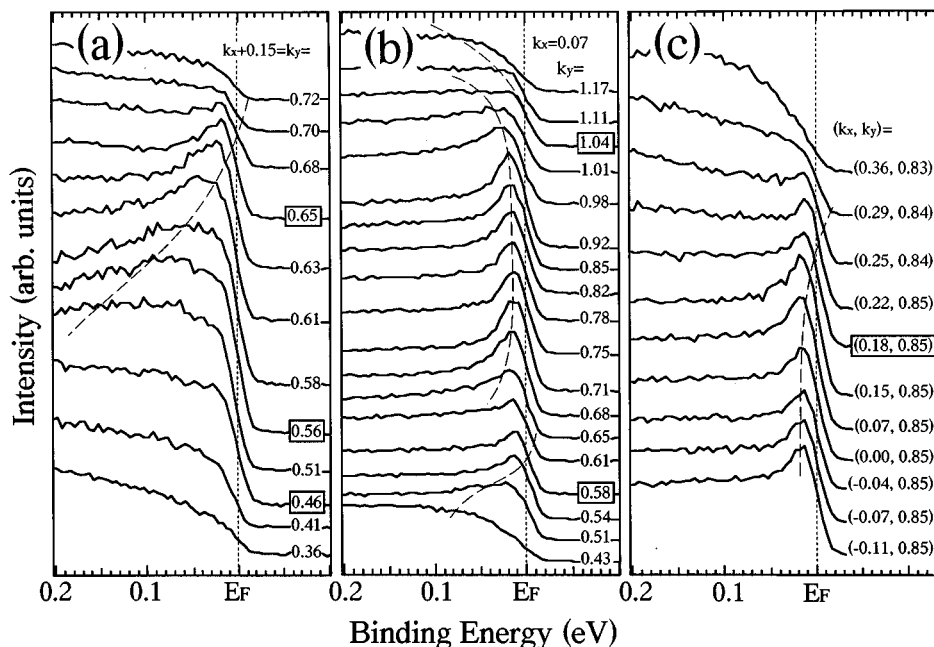

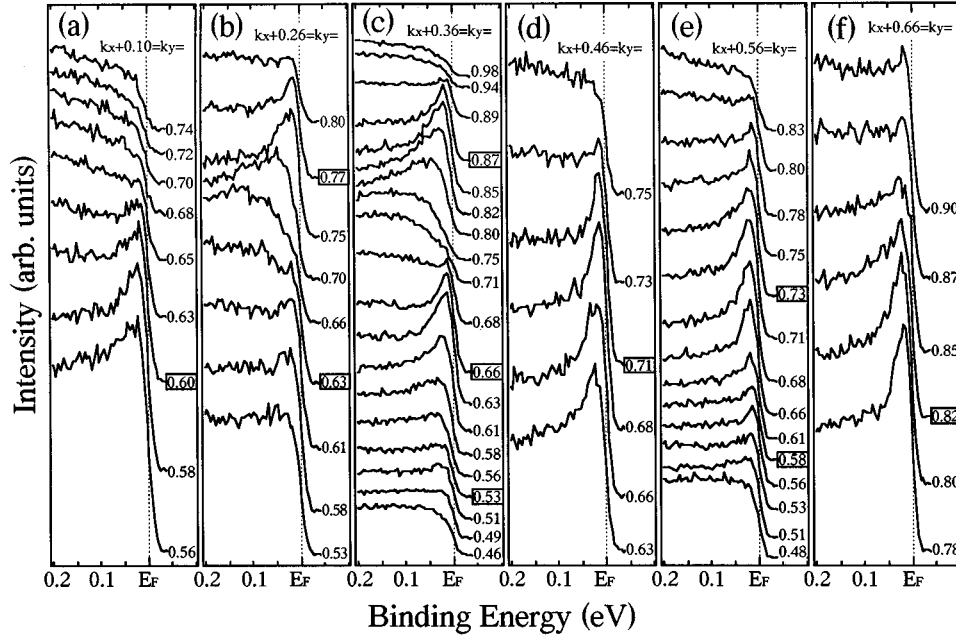FIG. 8. Same as Fig. 3, with an enlarged binding-energy scale.

FIG. 9. Six sets of HRARPES spectra near E_F along several cuts parallel to the ΓX direction measured at 13 K using 21.2-eV energy photons. The location of each cut in the Brillouin zone is shown in Fig. 4 using the figure number such as $9a$. The E_F-crossing points determined according to the criteria described in the text are marked by enclosing the wave vector on each ARPES spectrum with a box.

by the number, such as $9a$. Using the criteria described above, we determined several E_F-crossing points which are shown by filled circles in Fig. 4, and also by enclosing the wave vector denoted on each ARPES spectrum with a box in Figs. 8 and 9.

In Fig. 10 we plot the observed E_F-crossing points in the extended Brillouin zone using the symmetry of the crystal. The connection between the points is shown by different shadings (open, gray, and black). Broken lines show the Fermi surface predicted by the band calculation.[2] As is seen in Fig. 10, the observed Fermi surface consists of three Fermi-surface sheets; one electronlike sheet centered at the Γ point and two holelike sheets centered at the X point. In our
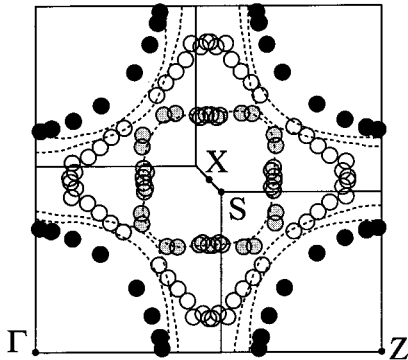

FIG. 10. The experimental Fermi surface of Sr_2RuO_4 obtained by the present HRARPES measurement (open, gray, and filled circles). It consists of one electronlike Fermi surface sheet centered at the Γ point (filled circles) and two holelike sheets centered at the X point (gray and open circles). The Fermi surface predicted by the band calculation (Ref. 2) (broken lines) is also shown for comparison.

previous ARPES study,[10] we observed the two holelike Fermi-surface sheets centered at the X point but could not resolve very well the electronlike sheet centered at the Γ point, probably due to the relatively lower energy resolution (50 meV). The higher-energy resolution (15–20 meV) in this study confirms the identification of the electronlike sheet centered at the Γ point as shown in Fig. 5.

There is good agreement between the measured and calculated holelike sheets, as shown in Fig. 10. The experimental electronlike Fermi surface sheet centered at the Γ point may correspond to one of two calculated electronlike sheets, probably, the smaller one. However, the area of the electronlike Fermi-surface sheet is considerably smaller in the experiment than in the calculation. The most remarkable difference between the experiment and the calculation is that one of the calculated electronlike Fermi-surface sheets centered at the Γ point appears to transform into a holelike sheet centered at the X point. This change directly relates to the appearance of the vHS around the middle point between the Γ and Z points, as seen in Fig. 10. Such a drastic change in the Fermi-surface topology could lead to a change of the electron count, as discussed by Singh.[3] However, the increased electron count due to the transformation of an electronlike sheet to a holelike one seems to be compensated by the shrinking of the electronlike sheet centered at the Γ point. Actually, when we estimated quantitatively the area between the two Fermi-surface topologies, we found that they are the same. This result seems consistent with a de Haas–van Alphen measurement, which also found three Fermi-surface sheets, reporting that the area of one Fermi-surface sheet decreases, while that of another increases in comparison with the band calculation.[22] However, they interpreted their data based on one holelike and two electronlike sheets, in contrast with the present HRARPES measurement. It is more likely

that the electron-electron correlations modify the band dispersion near E_F, and as a result give a different Fermi-surface topology with an extended vHS just below E_F. This explanation is consistent with several transport measurements[1,6–8] and the recent resonant photoemission study[9] which observed substantial correlation effects in Sr_2RuO_4.

IV. CONCLUSION

We have performed high-resolution (HR) ARPES studies on single crystals of Sr_2RuO_4. The valence-band ARPES spectra show three groups of dispersive bands; one near E_F, one around 3-eV binding energy, and the third at 6–8 eV binding energy. These groups are ascribed to the $Ru4d\varepsilon$-$O2p\pi$ antibonding bands, the $Ru4d\varepsilon$-$O2p\pi$ nonbonding bands, and the $Ru4d\varepsilon$-$O2p\pi$ bonding bands, respectively, in qualitative agreement with the band-structure calculation. However, HRARPES measurements taken in the vicinity of E_F show a narrower antibonding band compared to the band calculation, indicating the existence of correlation effects. More importantly, an extended vHS very close to E_F (with critical energy of 11 meV) is observed along the Ru-O bonding direction in analogy to the HTSC's, suggesting that an extended vHS may be a general feature of two-dimensional correlated metals. This result suggests a reexamination of the simple vHS scenario for the superconducting and normal-state properties of the HTSC's. It was also found that the vHS in Sr_2RuO_4 is more two-dimensional than that in the HTSC's. The Fermi-surface topology obtained by HRARPES (one electronlike sheet centered at the Γ point and two holelike sheets centered at the X point) is different from that of the band calculations (two electronlike sheets centered at the Γ point and one holelike sheet centered at the X point), although the electron count is the same in both cases. These results suggest an important role of electron correlations for understanding the electronic structure and properties of Sr_2RuO_4.

[1] Y. Maeno, H. Hashimoto, K. Yoshida, S. Nishizaki, T. Fujita, J. G. Bednorz, and F. Lichtenberg, Nature **372**, 532 (1995).

[2] T. Oguchi, Phys. Rev. B **51**, 1385 (1995).

[3] D. J. Singh, Phys. Rev. B **52**, 1358 (1995).

[4] L. F. Mattheiss, Phys. Rev. Lett. **58**, 1028 (1987).

[5] F. Lichtenberg, A. Catana, J. Mannhart, and D. G. Schlom, Appl. Phys. Lett. **60**, 1138 (1992).

[6] J. J. Neumeier, M. F. Hundley, M. G. Smith, J. D. Thompson, C. Allgeier, H. Xie, W. Yelon, and J. S. Kim, Phys. Rev. B **49**, 17 910 (1994).

[7] R. J. Cava, B. Batlogg, K. Kiyono, H. Takagi, J. J. Krajewski, W. F. Peck, Jr., L. W. Rupp, Jr., and C. H. Chen, Phys. Rev. B **49**, 11 890 (1994).

[8] S. A. Carter, B. Batlogg, R. J. Cava, J. J. Krajewski, W. F. Peck, Jr., and L. Rupp, Jr., Phys. Rev. B **51**, 17 184 (1995).

[9] T. Yokoya, A. Chainani, T. Takahashi, H. Katayama-Yoshida, M. Kasai, Y. Tokura, N. Shanthi, and D. D. Sarma, Phys. Rev. B **53**, 8151 (1996).

[10] T. Yokoya, A. Chainani, T. Takahashi, H. Katayama-Yoshida, M. Kasai, and Y. Tokura, Phys. Rev. Lett. **76**, 3009 (1996).

[11] D. M. King, Z.-X. Shen, D. S. Dessau, B. O. Wells, W. E. Spicer, A. J. Arko, D. S. Marshall, J. DiCarlo, A. G. Loeser, C. H. Park, E. R. Ratner, J. L. Peng, Z. Y. Li, and R. L. Greene, Phys. Rev. Lett. **70**, 3159 (1993).

[12] D. S. Dessau, Z.-X. Shen, D. M. King, D. S. Marshall, L. W. Lombardo, P. H. Dickinson, A. G. Loeser, J. DiCarlo, C.-H. Park, A. Kapitulnik, and W. E. Spicer, Phys. Rev. Lett. **71**, 2781 (1993).

[13] K. Gofron *et al.*, J. Phys. Chem. Solids **54**, 1193 (1993); A. A. Abrikosov, J. C. Campuzano, and K. Gofron, Physica C **214**, 73 (1993); K. Gofron *et al.*, Phys. Rev. Lett. **73**, 3302 (1994).

[14] D. M. King, Z.-X. Shen, D. S. Dessau, B. O. Well, W. E. Spicer, A. J. Arko, D. S. Marshall, J. Dicarlo, A. G. Loeser, C. H. Park, E. R. Ratner, J. L. Peng, Z. Y. Li, and R. L. Greene, Phys. Rev. Lett. **73**, 3298 (1994).

[15] Jian Ma, C. Quitmann, R. J. Kelley, P. Aimeras, H. Berger, G. Margaritondo, and M. Onellion, Phys. Rev. B **51**, 3832 (1995).

[16] J. M. Luttinger, Phys. Rev. **119**, 1153 (1960).

[17] A. Gulino, R. G. Egdell, P. D. Battle, and S. H. Kim, Phys. Rev. B **51**, 6827 (1995); P. A. Cox, R. G. Egdell, J. B. Goodenough, A. Hamnett, and C. C. Naish, J. Phys. C **16**, 6221 (1983).

[18] F. J. Himpsel, Adv. Phys. **32**, 1 (1983).

[19] T. Katsufuji, M. Kasai, and Y. Tokura, Phys. Rev. Lett. **76**, 126 (1996).

[20] H. Ding, A. F. Bellman, J. C. Campuzano, M. Randeria, M. R. Norman, T. Yokoya, T. Takahashi, H. Katayama-Yoshida, T. Mochiku, K. Kadowaki, G. Jennings, and G. P. Brivio, Phys. Rev. Lett. **76**, 1533 (1996).

[21] D. M. Newns, H. R. Krishnamurthy, P. C. Pattnaik, C. C. Tsuei, C. C. Chi, and C. L. Kane, Physica (Amsterdam) B **186**, 801 (1993).

[22] A. P. Mackenzie, S. R. Julian, A. J. Diver, G. J. McMullan, M. P. Ray, G. G. Lonzarich, Y. Maeno, S. Nishizaki, and T. Fujita, Phys. Rev. Lett. **76**, 3786 (1996).